Physica E 69 (2015) 349–353

Contents lists available at ScienceDirect

Physica E

journal homepage: www.elsevier.com/locate/physe

Tunneling induced transparency and giant Kerr nonlinearity in multiple quantum dot molecules

Si-Cong Tian [a,*], Ren-Gang Wan [b], En-Bo Xing [a,c], Jia-Min Rong [a,c], Hao Wu [a], Li-Jie Wang [a], Shi-Li Shu [a], Cun-Zhu Tong [a], Yong-Qiang Ning [a]

[a] State Key Laboratory of Luminescence and Applications, Changchun Institute of Optics, Fine Mechanics and Physics, Chinese Academy of Sciences, Changchun 130033, China
[b] School of Physics and Information Technology, Shaanxi Normal University, Xi'an 710062, China
[c] Graduate School of the Chinese Academy of Sciences, Beijing 100049, China

HIGHLIGHTS

- The analytic expression for linear and nonlinear susceptibility is obtained.
- The multiple tunneling couplings can induce multiple transparency windows.
- Different probe fields can acquire giant Kerr nonlinearity simultaneously.
- The giant Kerr nonlinearity can be combined with vanishing absorption.

ARTICLE INFO

Article history:
Received 24 October 2014
Received in revised form
6 February 2015
Accepted 8 February 2015
Available online 9 February 2015

Keywords:
Tunneling induced transparency
Kerr nonlinearity
Quantum dots molecules

ABSTRACT

The linear absorption and the Kerr nonlinearity of multiple quantum dots molecules controlled by the tunneling rather than the laser fields are investigated. The tunneling between the dots can induce multiple transparency windows. By varying the energy splitting of the excited states and the tunneling intensity, the width of the tunneling induced transparency windows can be narrowed. Within the narrowed transparency windows, the steep dispersion profile of the probe field makes it possible to enhance the Kerr nonlinearity. Therefore more than one probe fields with different frequencies can acquire giant Kerr accompanied by vanishing absorption simultaneously.

© 2015 Elsevier B.V. All rights reserved.

1. Introduction

The phenomenon of electromagnetically induced transparency (EIT), which bases on the laser induced atomic coherence, plays an important role in the interaction between light and matter [1–3]. Possible applications of EIT include gain without inversion, controlling of light, enhancement of nonlinearity [1–3], and so on. Experimentally, EIT has been observed in various mediums [4–7]. Also in four- or multiple-level atomic systems EIT has been studied [8–15].

Kerr nonlinearity, which corresponds to the refractive part of the third-order susceptibility in optical media, plays an important role in the field of nonlinear optics [16], and can be used for many interesting applications, such as self-focusing [17], self-phase modulation for generation of optical solitons [18], and cross-phase modulation for polarization phase gates [19]. Enhancement of Kerr nonlinearity has been demonstrated in various EIT systems (such as three-level [20,21], N [22,23], M [24] and four-level Λ [25] systems), because that EIT is capable of producing enhanced Kerr nonlinearity and suppressing the linear absorption [1–3]. Therefore, the large enhancement of nonlinear susceptibilities in EIT media leads to the study of nonlinear optics at low light levels [26–28].

On the other hand, quantum dots (QDs) have many advantages over atoms, and that is, large electric-dipole moments, high nonlinear optical coefficients, customized design and ease of integration. Therefore, QDs can be used for obtaining EIT [7,29] and high Kerr nonlinearly [30] *via* coupling lasers. Quantum dot molecules (QDMs) are systems composed of two or more closely spaced and interacting QDs, and can be fabricated by using self-assembled dot growth technology [31]. By applying the laser fields, transparency and slow solitons [32], and enhanced Kerr nonlinearity [33] can be

* Corresponding author.
E-mail addresses: tiansicong@ciomp.ac.cn (S.-C. Tian), tongcz@ciomp.ac.cn (C.-Z. Tong).

http://dx.doi.org/10.1016/j.physe.2015.02.007
1386-9477/© 2015 Elsevier B.V. All rights reserved.

obtained in QDMs. And it is also possible to induce quantum interference and coherence in QDMs only by the tunneling [34–36]. Therefore, QDMs with two or three dots can be used in the field of EIT [37,38] or tunneling induced transparency (TIT) [39], optical bistability [40,41], entanglement [42], resonance fluorescence spectrum [43], coherent population transfer [44], Kerr nonlinearity [45,46] and cavity transmission spectrum [47].

In this paper we investigate the linear absorption and the Kerr nonlinearity of a multiple QDMs coupled by tunneling instead of laser fields. In such system, tunneling between the dots can induce multiple TIT windows and enhancement of Kerr nonlinearity. With proper values of the energy splitting of the excited states and the tunneling intensity, giant Kerr nonlinearity accompanied by vanishing absorption can be realized. Compared with QDMs with two or three dots [45,46], one than one probe fields with different frequencies can acquire giant Kerr simultaneously.

2. Model and equations

We show the schematic of the setup of the multiple QDMs (the number of QDs is N) in Fig. 1(a). QD1 and QDn ($n = 2, 3, \ldots, N$) are coupled by the gate electrodes, so there is tunneling between QD1 and QDn. Without a gate voltage, the conduction-band electron levels are out of resonance and the electron tunneling between the QDs is very weak. While with a gate voltage, the conduction-band electron levels come close to resonance and the electron tunneling between the QDs is greatly enhanced. Because of the far off-resonant valence-band energy levels, the hole tunneling can be neglected. Then the schematic of the level configuration of the multiple-QDs can be drawn, as shown in Fig. 1(b). The ground state $|0\rangle$ has no excitations, and the exciton state $|1\rangle$ has one electron–hole pair in QD1. With a bias voltage, the tunneling coupling can make the electron tunnel from QD1 to the other QDs forming the indirect excitons, denote as state $|n\rangle$ ($n = 2, 3, \ldots, N$).

The Hamiltonian of the basis $\{|0\rangle, |1\rangle, |2\rangle, \ldots, |N\rangle\}$ under the rotating-wave and the electric-dipole approximations can be written as (assumption of $\hbar = 1$)

$$H_I = \begin{pmatrix} 0 & -\Omega_p & 0 & \ldots & 0 \\ -\Omega_p & \delta_p & -T_2 & \ldots & -T_N \\ 0 & -T_2 & \delta_p - \omega_{12} & \ldots & 0 \\ \vdots & \vdots & \vdots & \vdots & \vdots \\ 0 & -T_n & 0 & \ldots & \delta_p - \omega_{1N} \end{pmatrix}. \quad (1)$$

here $\Omega_p = \mu_{01} E_p$ is the Rabi frequency of the transition $|0\rangle \to |1\rangle$. E_p denotes the electric-field amplitude of the laser, and $\mu_{01} = \boldsymbol{\mu}_{01}\cdot\mathbf{e}$ denotes electric dipole moment for the excitonic transition between states $|0\rangle$ and $|1\rangle$, with $\mathbf{e}$ being the polarization vector. T_n ($n = 2, 3, \ldots, N$) are the tunneling couplings, which depend on the barrier characteristics and the external electric field. $\delta_p = \omega_{10} - \omega_p$ is the detuning of the probe field, with ω_{10} being the transition frequency between $|1\rangle$ and $|0\rangle$ states. ω_{1n} ($n = 2, 3, \ldots, N$) is the energy splitting of the excited states, and can be controlled by manipulation of the external electric field that changes the effective confinement potential.

The state vector at any time t is

$$|\Psi_I(t)\rangle = \sum_{n=0}^{N} a_n(t)|n\rangle. \quad (2)$$

The evolution of the state vector obeys the Schrödinger equation

$$\frac{d}{dt}|\Psi_I(t)\rangle = -iH_I(t)|\Psi_I(t)\rangle. \quad (3)$$

Substituting Eqs. (1) and (2) into Eq. (3), and then using the Weisskopf–Wigner theory [48,49], the dynamical equations for atomic probability amplitudes in the interaction picture can be obtained:

$$i\dot{a}_0 = -\Omega_p a_1, \quad (4a)$$

$$i\dot{a}_1 = -\Omega_p a_0 - \sum_{n=2}^{N} T_n a_n + \left(\delta_p - i\gamma_1\right) a_1, \quad (4b)$$

$$i\dot{a}_n = -T_n a_1 + \left(\delta_p - \omega_{1n} - i\gamma_n\right) a_n \quad (n = 2, 3, \ldots, N), \quad (4c)$$

$$\sum_{n=0}^{N} |a_n|^2 = 1. \quad (4d)$$

here $\gamma_n = (1/2)\Gamma_{n0} + \gamma_{n0}^{d}$ ($n = 1, 2, 3, \ldots, N$) is the typical effective decay rate, with Γ_{n0} being the radiative decay rate of populations from $|n\rangle \to |0\rangle$ and γ_{n0}^{d} being the pure dephasing rates.

It is well known that the multiple-QDs media to the probe field is

$$P = \varepsilon_0 \chi_p E_p = \frac{\Gamma}{V}\mu_{01} a_1 a_0^{*}, \quad (5)$$

with Γ being the optical confinement factor, V being the volume of single QD, ε_0 being the dielectric constant [29]. From Eq. (5) the probe susceptibility can be obtained, which is given by

$$\chi_p = \frac{\Gamma}{V}\frac{\mu_{01}^2}{\varepsilon_0 \hbar \Omega_p} a_1 a_0^{*} = \frac{\Gamma}{V}\frac{\mu_{01}^2}{\varepsilon_0 \hbar}\chi. \quad (6)$$

In the steady state, we solve Eqs. (4) under the weak field approximation $\left(|a_0|^2 = 1\right)$, then (see Appendix A)

$$\chi = \frac{1}{\Gamma_1 - \sum_{n=2}^{N}(T_n^2/\Gamma_n)} \frac{1}{1 + \frac{\Omega_p^2}{\left|\Gamma_1 - \sum_{n=2}^{N}(T_n^2/\Gamma_n)\right|^2}\left(1 + \sum_{n=2}^{N}(T_n^2/|\Gamma_n|^2)\right)}, \quad (7)$$

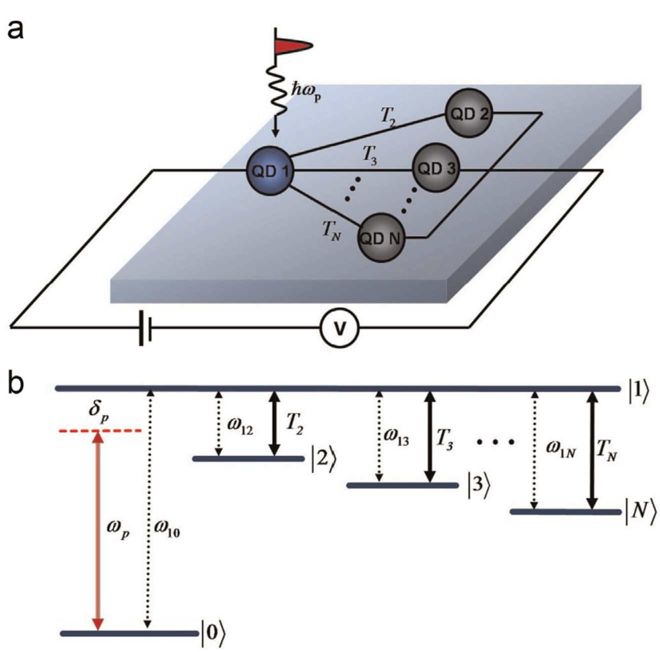

Fig. 1. (a) The schematic of the setup of a multiple QDMs. The probe field transmits the QD 1. The wavelengths of the probe field depends on the sample structure, and it could be around 870 nm according to Ref. [36]. V is a bias voltage, which is supposed to be several hundreds millivolt [31,35]. (b) The schematic of the level configuration of a multiple QDMs.

where $\Gamma_1 = \delta_p - i\gamma_1$ and $\Gamma_n = \delta_p - \omega_{1n} - i\gamma_n (n = 2, 3, \ldots N)$. Using Maclaurin formula and expending χ into the second order of Ω_p, then

$$\chi = \chi^{(1)} + \chi^{(3)}\Omega_p{}^2, \tag{8}$$

where $\chi^{(1)}$ and $\chi^{(3)}$ correspond to the first-order linear and third-order Kerr nonlinear parts of the susceptibility, respectively, and they are given by

$$\chi^{(1)} = \frac{1}{\Gamma_1 - \sum_{n=2}^{N} (T_n^2/\Gamma_n)}, \tag{9a}$$

$$\chi^{(3)} = -\frac{1}{\Gamma_1 - \sum_{n=2}^{N} (T_n^2/\Gamma_n)} \frac{1}{\left|\Gamma_1 - \sum_{n=2}^{N} (T_n^2/\Gamma_n)\right|^2} \left(1 + \sum_{n=2}^{N} \frac{T_n^2}{|\Gamma_n|^2}\right). \tag{9b}$$

3. Results and discussions

In this section, we will investigate the linear absorption $\mathrm{Im}\left[\chi^{(1)}\right]$ and Kerr nonlinearity $\mathrm{Re}\left[\chi^{(3)}\right]$ of multiple QDMs as a function of probe detuning for varying values of tunneling and energy splitting. For instance, we consider multiple QDMs with five dots. In such system, the tunneling coupling is $T_i (i = 2, 3, 4, 5)$, and the energy splitting of the excited levels is $\omega_{1i} (i = 2, 3, 4, 5)$. For simplicity, we only consider the case of $-\omega_{12} = \omega_{15}$ and $-\omega_{13} = \omega_{14}$. The realistic parameters are according to Ref. [39] and are scaled by the decay rate γ_1.

First we consider the case of none of the energy splitting being equal ($\omega_{12} \neq \omega_{13} \neq \omega_{14} \neq \omega_{15}$). Fig. 2 shows the linear absorption $\mathrm{Im}\left[\chi^{(1)}\right]$ (dotted line) and Kerr nonlinearity $\mathrm{Re}\left[\chi^{(3)}\right]$ (solid line) as a function of probe detuning for varying values of energy splitting. For equal intensity of tunneling, the absorption spectrum is symmetrical with five absorption peaks and four TIT windows. With $-\omega_{13} = \omega_{14} = 0.8$, the inner pair of absorption peaks are narrowed. In the area of the pair of narrow absorption peaks, the Kerr nonlinearity is greatly enhanced (Fig. 2(a)). When the energy splitting ω_{13} and ω_{14} are decreased to 0.4, there is no narrow absorption peak and the enhanced Kerr nonlinearity vanishes, as shown in Fig. 2(b). With small energy splitting ω_{13} and ω_{14} (*i.e.* $-\omega_{13} = \omega_{14} = 0.2$), the linewidth of the center absorption peak becomes narrowed. And in the area of the narrow absorption peak, the giant Kerr nonlinearity is acquired (Fig. 2(c)).

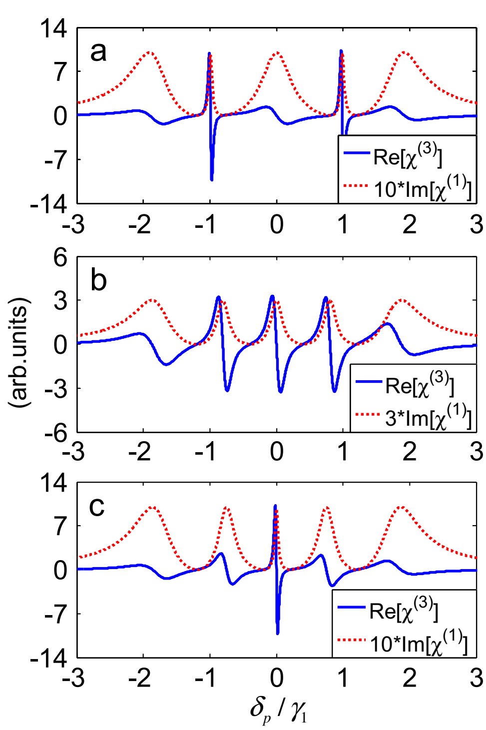

Fig. 2. Variation of $\mathrm{Re}\left[\chi^{(3)}\right]$ (solid line) and $\mathrm{Im}\left[\chi^{(1)}\right]$ (dotted line) of QDMs (the number of the dots is five) as a function of the probe detuning δ_p for different energy splitting ω_{13} and ω_{14}: (a) $-\omega_{13} = \omega_{14} = 0.8$, (b) $-\omega_{13} = \omega_{14} = 0.4$, (c) $-\omega_{13} = \omega_{14} = 0.2$. Other parameters are $-\omega_{12} = \omega_{15} = 1.2$, $T_2 = T_3 = T_4 = T_5 = 0.8$, $\gamma_1 = 1$, $\gamma_2 = \gamma_3 = \gamma_4 = \gamma_5 = 10^{-3}$.

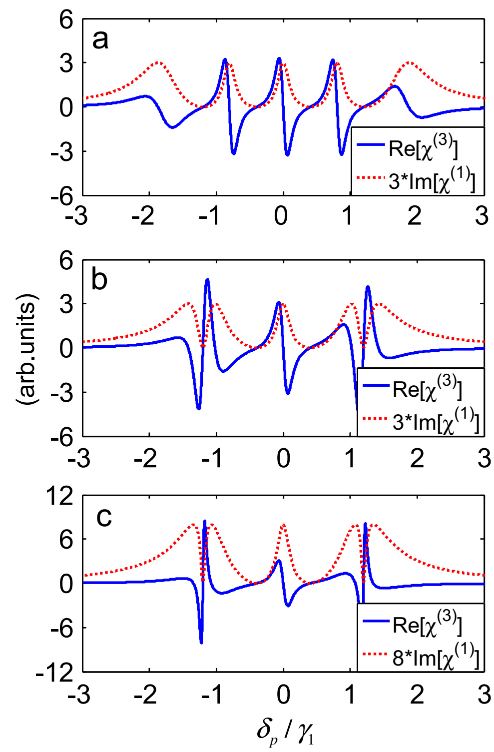

Fig. 3. Variation of $\mathrm{Re}\left[\chi^{(3)}\right]$ (solid line) and $\mathrm{Im}\left[\chi^{(1)}\right]$ (dotted line) of QDMs (the number of the dots is five) as a function of the probe detuning δ_p for different tunneling intensity T_2 and T_5: (a) $T_2 = T_5 = 0.8$, (b) $T_2 = T_5 = 0.3$, (c) $T_2 = T_5 = 0.2$. Other parameters are $T_3 = T_4 = 0.8$, $-\omega_{12} = \omega_{15} = 1.2$, $-\omega_{13} = \omega_{14} = 0.4$, $\gamma_1 = 1$, $\gamma_2 = \gamma_3 = \gamma_4 = \gamma_5 = 10^{-3}$.

In Fig. 2, though the Kerr nonlinearity is enhanced, it is accompanied by a strong linear absorption, which is not desirable for applications of low intensity nonlinear optics. Fortunately, one can tune the tunneling intensity to obtain the enhanced Kerr nonlinearity with vanishing absorption. Fig. 3 shows the linear absorption $\mathrm{Im}\left[\chi^{(1)}\right]$ (dotted line) and Kerr nonlinearity $\mathrm{Re}\left[\chi^{(3)}\right]$ (solid line) as a function of probe detuning for varying values of tunneling intensity T_2 and T_5. It can be seen that the linear absorption spectrum is symmetrical with five absorption peaks and four TIT windows (dotted line). As T_2 and T_5 are both decreasing, the outer pair of TIT windows become narrowed. And within the narrowed TIT windows, the Kerr nonlinearity $\mathrm{Re}\left[\chi^{(3)}\right]$ is greatly enhanced (Fig. 3(c)). This means that two probe fields with different frequencies can simultaneously acquire giant Kerr nonlinearity with suppressed linear absorption.

From the results obtained in Figs. 2 and 3, it can be concluded that the linear absorption and the Kerr nonlinearity can be controlled by the energy splitting and the tunneling intensity. Within the narrow absorption peaks or the narrow TIT windows, the steep dispersion profile of the probe field makes it possible to enhance

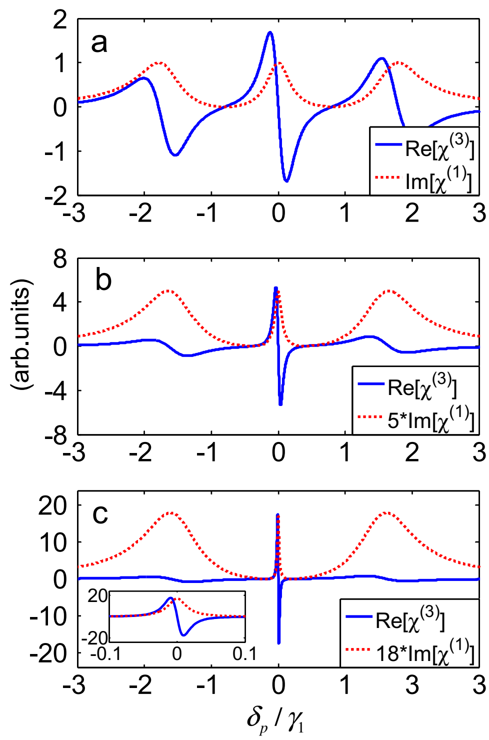

Fig. 4. Variation of Re$\left[\chi^{(3)}\right]$ (solid line) and Im$\left[\chi^{(1)}\right]$ (dotted line) of QDMs (the number of the dots is five) as a function of the probe detuning δ_p for different energy splitting: (a) $-\omega_{12} = -\omega_{13} = \omega_{14} = \omega_{15} = 0.8$, (b) $-\omega_{12} = -\omega_{13} = \omega_{14} = \omega_{15} = 0.4$, (c) $-\omega_{12} = -\omega_{13} = \omega_{14} = \omega_{15} = 0.2$. Other parameters are $T_2 = T_3 = T_4 = T_5 = 0.8$, $\gamma_1 = 1$, $\gamma_2 = \gamma_3 = \gamma_4 = \gamma_5 = 10^{-3}$.

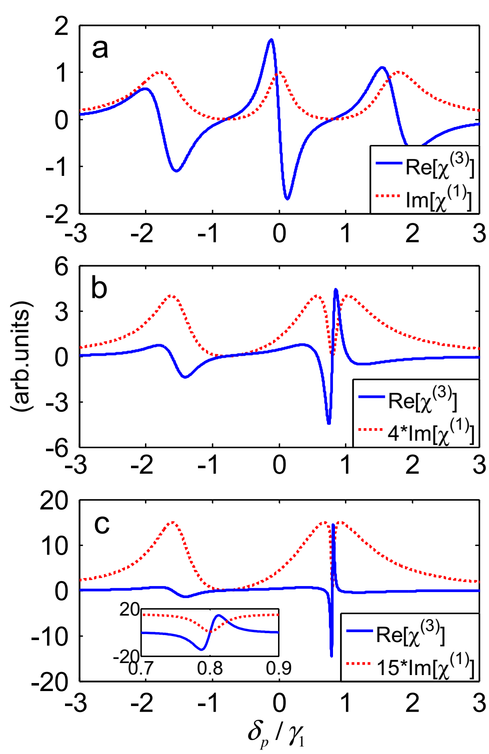

Fig. 5. Variation of Re$\left[\chi^{(3)}\right]$ (solid line) and Im$\left[\chi^{(1)}\right]$ (dotted line) of QDMs (the number of the dots is five) as a function of the probe detuning δ_p for different tunneling intensity T_4 and T_5: (a) $T_4 = T_5 = 0.8$, (b) $T_4 = T_5 = 0.2$, (c) $T_4 = T_5 = 0.1$. Other parameters are $T_2 = T_3 = 0.8$, $-\omega_{12} = -\omega_{13} = \omega_{14} = \omega_{15} = 0.8$, $\gamma_1 = 1$, $\gamma_2 = \gamma_3 = \gamma_4 = \gamma_5 = 10^{-3}$.

the Kerr nonlinearity. And in the later case, giant Kerr nonlinearity with vanishing absorption can be achieved. Compared with QDMs with two or three dots [45,46], in multiple QDMs Kerr nonlinearity can be greatly enhanced for probe fields with different frequencies.

The above investigations are made in the condition of $\omega_{12} \neq \omega_{13} \neq \omega_{14} \neq \omega_{15}$. In the following, we will consider the case of $-\omega_{12} = -\omega_{13} = \omega_{14} = \omega_{15} = \omega$. In Fig. 4 we plot the linear absorption Im$\left[\chi^{(1)}\right]$ (dotted line) and Kerr nonlinearity Re$\left[\chi^{(3)}\right]$ (solid line) as a function of probe detuning for varying values of ω. When the tunneling intensities are equal, the linear absorption spectrum is symmetrical. However, compared with the above results, there are only three absorption peaks and two TIT windows. With decreasing values of energy splitting ω, the linewidth of the center peak becomes much narrower. Simultaneously the Kerr nonlinearity is greatly enhanced within the narrower absorption peak, but it is accompanied by a strong linear absorption (Fig. 4(c)).

In order to overcome this disadvantage, we change the tunneling intensity T_4 and T_5, and show the corresponding results in Fig. 5. As can be seen from dotted line, when the tunneling intensities are not equal, the linear absorption spectrum becomes unsymmetrical, but still with three absorption peaks and two TIT windows [dotted line]. With decreasing values of T_4 and T_5, the TIT window on the right side becomes narrowed, and simultaneously the Kerr nonlinearity Re$\left[\chi^{(3)}\right]$ is enhanced and gradually enters the narrowed TIT window (Fig. 5(c)). That is to say, the Kerr nonlinearity is dramatically enhanced with suppressed linear absorption.

From the results obtained in Figs. 4 and 5, it can be concluded that when some of the energy splittings are equal, the number of the linear absorption peaks and the TIT windows is reduced. Within the narrow absorption peak or the narrow TIT window, the steep dispersion profile of the probe field can also enhance the Kerr nonlinearity. And within the narrow TIT window, giant Kerr nonlinearity is obtained with vanishing absorption.

4. Conclusions

In this paper, we have studied the multiple QDMs under the tunneling couplings and obtained a general analytic expression for linear and nonlinear susceptibility of the probe field. The results show that the absorption spectrum can exhibit multiple TIT windows and the Kerr nonlinearity can be enhanced. By changing the energy splitting and the tunneling intensity, the probe fields with different frequencies can acquire giant Kerr nonlinearity accompanied by vanishing absorption at the same time. Potential applications of such semiconductor nanostructures are to the enhancement of self-phase modulation at low light levels, such as optical solitons and self-focusing.

Acknowledgments

This work is supported by the financial support from the National Natural Science Foundation of China, China (Grant nos. 11304308 and 61176046), the National Basic Research Program of China (Grant no. 2013CB933300), the International Science Technology Cooperation Program of China (No. 2013DFR00730), the Hundred Talents Program of Chinese Academy of Sciences, and the Natural Science Foundation of Jilin Province (Grant no. 20140101203JC).

Appendix A

The analytical expressions of the first and third order susceptibilities can be obtained by solving Eqs. (4). Under the steady-state condition $\left(|a_0|^2 = 1\right)$, Eqs. (4a)–(4d) go to

$$-\Omega_p a_1 = 0, \tag{A1a}$$

$$-\Omega_p a_0 - \sum_{n=2}^{N} T_n a_n + \Gamma_1 a_1 = 0, \tag{A1b}$$

$$-T_n a_1 + \Gamma_n a_n = 0 \quad (n = 2, 3, \ldots, N), \tag{A1c}$$

$$\sum_{n=0}^{N} |a_n|^2 = 1, \tag{A1d}$$

with $\Gamma_1 = \delta_p - i\gamma_1$ and $\Gamma_n = \delta_p - \omega_{1n} - i\gamma_n \quad (n = 2, 3, \ldots, N)$.

From (A1c),

$$a_n = \frac{T_n}{\Gamma_n} a_1. \tag{A2}$$

Substituting Eq. (A2) into Eq. (A1b), then

$$a_1 = \Omega_p \frac{1}{\Gamma_1 - \sum_{n=2}^{N} \frac{T_n^2}{\Gamma_n}} a_0. \tag{A3}$$

Substituting Eqs. (A2) and (A3) into Eq. (A1d), then

$$|a_0|^2 = \frac{1}{1 + \frac{\Omega_p^2}{\left|\Gamma_1 - \sum_{n=2}^{N} \frac{T_n^2}{\Gamma_n}\right|^2}\left(1 + \sum_{n=2}^{N} \frac{T_n^2}{|\Gamma_n|^2}\right)}. \tag{A4}$$

The coherence element between state $|0\rangle$ and $|1\rangle$ is

$$a_1 a_{0^*} = \Omega_p \frac{1}{\Gamma_1 - \sum_{n=2}^{N} \frac{T_n^2}{\Gamma_n}} |a_0|^2. \tag{A5}$$

Substituting Eq. (A4) into Eq. (A5), then

$$\chi = \frac{a_1 a_{0^*}}{\Omega_p} = \frac{1}{\Gamma_1 - \sum_{n=2}^{N} \frac{T_n^2}{\Gamma_n}} \frac{1}{1 + \frac{\Omega_p^2}{\left|\Gamma_1 - \sum_{n=2}^{N} \frac{T_n^2}{\Gamma_n}\right|^2}\left(1 + \sum_{n=2}^{N} \frac{T_n^2}{|\Gamma_n|^2}\right)}. \tag{A6}$$

Using the Maclaurin formula and expand χ into the second order of Ω_p, then

$$\chi = \frac{1}{\Gamma_1 - \sum_{n=2}^{N} \frac{T_n^2}{\Gamma_n}} \left[1 - \frac{\Omega_p^2}{\left|\Gamma_1 - \sum_{n=2}^{N} \frac{T_n^2}{\Gamma_n}\right|^2}\left(1 + \sum_{n=2}^{N} \frac{T_n^2}{|\Gamma_n|^2}\right)\right]. \tag{A7}$$

The first order susceptibilities is proportional to $\Omega_p^{(0)}$, and the third order susceptibilities is proportional to Ω_p^2, thus

$$\chi = \chi^{(1)} + \chi^{(3)} \Omega_p^2, \tag{A8}$$

with

$$\chi^{(1)} = \frac{1}{\Gamma_1 - \sum_{n=2}^{N} \frac{T_n^2}{\Gamma_n}}, \tag{A9a}$$

$$\chi^{(3)} = -\frac{1}{\Gamma_1 - \sum_{n=2}^{N} \frac{T_n^2}{\Gamma_n}} \frac{1}{\left|\Gamma_1 - \sum_{n=2}^{N} \frac{T_n^2}{\Gamma_n}\right|^2}\left(1 + \sum_{n=2}^{N} \frac{T_n^2}{|\Gamma_n|^2}\right). \tag{A9b}$$

References

[1] S.E. Harris, Phys. Today 50 (1997) 36.
[2] J.P. Marangos, J. Mod. Opt. 45 (1998) 471.
[3] M. Fleischhauer, A. Imamoglu, J.P. Marangos, Rev. Mod. Phys. 77 (2005) 633.
[4] K.J. Boller, A. Imamolu, S.E. Harris, Phys. Rev. Lett. 66 (1991) 2593.
[5] B.S. Ham, P.R. Hemmer, M.S. Shahriar, Opt. Commun. 144 (1997) 227.
[6] G.B. Serapiglia, E. Paspalakis, C. Sirtori, K.L. Vodopyanov, C.C. Phillips, Phys. Rev. Lett. 84 (2000) 1019.
[7] S. Marcinkevičius, A. Gushterov, J.P. Reithmaier, Appl. Phys. Lett. 92 (2008) 041113.
[8] E.A. Korsunsky, N. Leinfellner, A. Huss, S. Baluschev, L. Windholz, Phys. Rev. A 59 (1999) 2302.
[9] M.D. Lukin, S.F. Yelin, M. Fleischhauer, M.O. Scully, Phys. Rev. A 60 (1999) 3225.
[10] Y.C. Chen, Y.A. Liao, H.Y. Chiu, J.J. Su, I.A. Yu, Phys. Rev. A 64 (2001) 053806.
[11] M. Yan, E.G. Rickey, Y. Zhu, Phys. Rev. A 64 (2001) 013412.
[12] E. Paspalakis, P.L. Knight, Phys. Rev. A 66 (2002) 015802.
[13] E. Paspalakis, P.L. Knight, J. Opt. B: Quantum Semiclass. Opt. 4 (2002) S372.
[14] C.L. Wang, A.J. Li, X.Y. Zhou, Z.H. Kang, J. Yun, J.Y. Gao, Opt. Lett. 33 (2008) 687.
[15] S.C. Tian, Z.H. Kang, C.L. Wang, R.G. Wan, J. Kou, H. Zhang, Y. Jiang, H.N. Cui, J. Y. Gao, Opt. Commun. 285 (2012) 294.
[16] R.W. Boyd, Nonlinear Optics, Academic, New York, 1992.
[17] S. Chi, Q. Guo, Opt. Lett. 20 (1995) 1598.
[18] V. Tikhonenko, J. Christou, B. Luther-Davies, Phys. Rev. Lett. 76 (1996) 2698.
[19] S. Rebić, D. Vitali, C. Ottaviani, P. Tombesi, M. Artoni, F. Cataliotti, R. Corbalán, Phys. Rev. A 70 (2004) 032317.
[20] S.E. Harris, J.E. Field, A. Imamoğlu, Phys. Rev. Lett. 64 (1990) 1107.
[21] H. Wang, D. Goorskey, M. Xiao, Phys. Rev. Lett. 87 (2001) 073601.
[22] H. Schmidt, A. Imamoglu, Opt. Lett. 21 (1996) 1936.
[23] H. Kang, Y. Zhu, Phys. Rev. Lett. 91 (2003) 093601.
[24] A.B. Matsko, I. Novikova, G.R. Welch, M.S. Zubairy, Opt. Lett. 28 (2003) 96.
[25] Y. Niu, S. Gong, R. Li, Z. Xu, X. Liang, Opt. Lett. 30 (2005) 3371.
[26] P.R. Hemmer, D.P. Katz, J. Donoghue, M.S. Shahriar, P. Kumar, M. Cronin-Golomb, Opt. Lett. 20 (1995) 982.
[27] A. Imamoğlu, H. Schmidt, G. Woods, M. Deutsch, Phys. Rev. Lett. 79 (1997) 1467.
[28] S.E. Harris, L.V. Hau, Phys. Rev. Lett. 82 (1999) 4611.
[29] J. Kim, S.L. Chuang, P.C. Ku, C.J. Chang-Hasnain, J. Phys.: Condens. Matter 16 (2004) S3727.
[30] A.H. Al-Khursan, M.K. Al-Khakani, K.H. Al-Mossawi, Photon. Nanostruct. 7 (2009) 153.
[31] L. Wang, A. Rastelli, S. Kiravittaya, M. Benyoucef, O.G. Schmidt, Adv. Mater. 21 (2009) 2601.
[32] Y.C. She, X.J. Zheng, D.L. Wang, W.X. Zhang, Opt. Express 21 (2013) 17392.
[33] B. Al-Nashy, S.M.M. Amin, Amin H. Al-Khursan, J. Opt. Soc. Am. B 31 (2014) 1991.
[34] K. Müller, A. Bechtold, C. Ruppert, M. Zecherle, G. Reithmaier, M. Bichler, H. J. Krenner, G. Abstreiter, A.W. Holleitner, J.M. Villas-Boas, M. Betz, J.J. Finley, Phys. Rev. Lett. 108 (2012) 197402.
[35] K.M. Weiss, J.M. Elzerman, Y.L. Delley, J. Miguel-Sanchez, A. Imamoğlu, Phys. Rev. Lett. 109 (2012) 107401.
[36] N. Sköld, A. Boyer de la Giroday, A.J. Bennett, I. Farrer, D.A. Ritchie, A.J. Shields, Phys. Rev. Lett. 110 (2013) 016804.
[37] C.H. Yuan, K.D. Zhu, Appl. Phys. Lett. 89 (2006) 052115.
[38] S. Michael, W.W. Chow, H.C. Schneider, Phys. Rev. B 88 (2013) 125305.
[39] H.S. Borges, L. Sanz, J.M. Villas-Bôas, O.O. Diniz Neto, A.M. Alcalde, Phys. Rev. B 85 (2012) 115425.
[40] J. Li, R. Yu, J. Liu, P. Huang, X. Yang, Physica E 41 (2008) 70.
[41] S.C. Tian, R.G. Wan, C.Z. Tong, Y.Q. Ning, J. Opt. Soc. Am. B 31 (2014) 2681.
[42] X.Y. Lü, J. Wu, L.L. Zheng, Z.M. Zhan, Phys. Rev. A 83 (2011) 042302.
[43] S.C. Tian, R.G. Wan, C.Z. Tong, Y.Q. Ning, L. Qin, Y. Liu, J. Phys. B: At. Mol. Opt. Phys. 47 (2014) 155503.
[44] E. Voutsinas, A.F. Terzis, E. Paspalakis, Phy. Lett. A 378 (2014) 219.
[45] Y.D. Peng, A.H. Yang, D.H. Li, H. Zhang, Y.P. Niu, S.Q. Gong, Laser Phys. Lett. 11 (2014) 065201.
[46] S.C. Tian, R.G. Wan, C.Z. Tong, Y.Q. Ning, L. Qin, Y. Liu, J. Opt. Soc. Am. B 31 (2014) 1436.
[47] S.C. Tian, R.G. Wan, L.H. Li, C.Z. Tong, Y.Q. Ning, Opt. Commun. 334 (2015) 94.
[48] G.S. Agarwal, Quantum Optics, Springer-Verlag, Berlin, 1974.
[49] S.M. Radmore, P.M. Radmore, Methods in Theoretical Quantum Optics, Oxford University Press, Oxford, 1997.